Active Removal of Large Massive Objects by Hybrid Propulsion Module

L.T. DeLuca, M. Lavagna*, F. Maggi*, P. Tadini*, C. Pardini**, L. Anselmo**, M. Grassi***, U. Tancredi****, A. Francesconi*****,F. Branz*****, S. Chiesa******, N. Viola******, V. Trushlyakov********

**Politecnico di Milano, Milan, Italy*

Via La Masa 34, 20156 Milan, Italy

***Space Flight Dynamics Laboratory, ISTI/CNR, Pisa, Italy*

Via G. Moruzzi 1, 56124 Pisa, Italy

****Università Filippo II di Napoli, Naples, Italy*

Piazzale Tecchio 80, 80125Naples, Italy

*****Dipartimento delle Tecnologie Università di Napoli Parthenope, Naples, Italy*

Via Ammiraglio Ferdinando Acton 38, 80133 Naples, Italy

******CISAS Università di Padova, Padua, Italy*

Via Venezia 15, 35131 Padua, Italy

*******Politecnico di Torino, Turin, Italy*

Corso Duca degli Abruzzi 24, 10129 Turin, Italy

********Omsk State Technical University, Omsk, Russian Federation*

Pr. Mira 11, 644050 Omsk, RussianFederation

Abstract

This paper deals with the feasibility study of a mission for the active removal of a large massive object, such as the second stage of the Zenit launcher or the Envisat spacecraft, abandoned in the most populated orbit region in low Earth orbit. Critical mission aspects and related technologies are investigated at a preliminary level. In particular, an innovative electro-adhesive system for target capture, mechanical systems for chaser-debris hard docking and a hybrid propulsion module for rendezvous and controlled de-orbiting and reentry are analyzed. A preliminary mass budget for the needed chaser platform and hybrid propulsion module is also performed, showing that the chaser spacecraft overall mass varies in the range 1500-1700 kg, with the propulsion module weighting about 900 kg.

1. Introduction

As of 14 May 2013, 3738 payloads and 1965 rocket bodies orbit the Earth [1]. Taking into account that approximately 1050 spacecraft are operational [2], there are around 4650 intact payloads and rocket bodies abandoned in the circumterrestrial space. In Low Earth Orbit (LEO), i.e. below the altitude of 2000 km, where the orbital object and debris density is maximum, there are 1939 payloads and 813 rocket bodies, of which about 2250 are completely abandoned. Therefore, more than 48% of the intact spacecraft and upper stages reside entirely in LEO, and this also applies to the abandoned objects.

The total mass in orbit as of 14 May 2013, extrapolated from [3] and [4], is around 6670 metric tons, including the International Space Station (420 metric tons). It is mainly concentrated in spacecraft (53.3%) and upper stages (42.5%), while mission related objects account for only 2.5% and orbital fragments for 1.7%. Excluding the International Space Station (ISS), the total mass in LEO is approximately 2650 metric tons, of which about 97% concentrated in payloads and rocket bodies. Overall, the average payload mass is 950 kg, ISS included, and 838 kg, ISS excluded, while rocket bodies have an average mass of 1442 kg. Ignoring the ISS, the average mass of intact spacecraft and upper stages currently in space is 1046 kg, reduced to 934 kg for the objects entirely resident in LEO, i.e. with a mean altitude lower than 2000 km.

During the last decade, several detailed parametric simulations have shown that the most effective way to prevent the further long-term growth of debris larger than 10 cm, able to cause the catastrophic collisional breakup of an "average" 934 kg object in LEO, would be to remove mass from densely populated orbital regimes, in addition to the strict adoption of recommended mitigation guidelines [5]. In practice, the active yearly removal of approximately 0.2–0.5% of the abandoned intact objects in LEO would be sufficient, provided that the highest priority were given to the targets characterized by the highest products of catastrophic collision probability with debris (P_c) and target mass (M), i.e. $P_c \times M$ [4][6]. Hybrid rocket technology is a valuable option [7], as discussed in detail in section 5. The active debris removal by means of a Hybrid Propulsion Module (HPM) aims at achieving contact and control of massive large abandoned objects, which have then to be removed. The chaser spacecraft in charge of this function includes the capture and mating kit, an HPM as primary propulsion system and monopropellant secondary propulsion for the attitude control, as well as the required avionics for this kind mission.

2. Target selection

Representing a potential source of hundreds or thousands of breakup fragments larger than 10 cm, posing an additional collision risk,the optimal targets for active removal should be large intact objects in crowded LEO regions characterized by significant orbital lifetimes (L_T). They can be ranked according to [8]:

$$R \propto P_c \times M^{0.75} \quad \textbf{(1)}$$

where the mass exponent 0.75 reproduces the trend of the cumulative number N of catastrophic collision fragments larger than a given characteristic size L (expressed in meters), according to the NASA standard breakup model [9][10]:

$$N(L) = 0.1\, M^{0.75} L^{-1.71} \quad \textbf{(2)}$$

In Eq. (2), M (expressed in kg) represents the cumulative mass of the target object and impacting debris, but in practice it is very close to the target mass, being the latter typically much larger (by 3 orders of magnitude in LEO) than the impactor's one. Being $P_c << 1$, the probability of catastrophic collision can be expressed as:

$$P_c \propto F(h,i,\, M)\, A L_T \quad \textbf{(3)}$$

where $F(h,i,\, M)$ is the average flux of debris leading to catastrophic breakup and A is the target average cross-section. For nearly circular orbits in LEO, $F(h,i,\, M)$ is a function of the orbit inclination i and the slowly decaying mean altitude h. In addition, over the 0.2–5.0 kg mass range of impactors able to destroy intact objects, $F(h,i,\, M)$ slightly decreases if the target mass M increases, because a more massive projectile is needed to completely shatter a higher mass target and the cumulative number of debris above a certain mass declines as the threshold moves to greater values. The residual lifetime of LEO objects in nearly circular orbits subjected to thermospheric drag may be approximated as $L_T \propto M/A$ [11], so Eq. (1) can be rewritten as follows:

$$R \propto F(h,i,\, M)\, A\, (M/A)\, M^{0.75} = F(h,i,\, M)\, M^{1.75} \quad \textbf{(4)}$$

Therefore, for abandoned objects subjected to comparable fluxes of debris able to cause catastrophic fragmentations, the applicable ranking for optimal removal can be reasonably considered proportional to$M^{1.75}$, so the target mass plays a very relevant role. In other words, in a crowded region of space in LEO, the removal of high mass objects is much more beneficial, for the long-term debris environment, than the withdrawal of average, or below the average, objects. In addition, due to the observed mass distribution among spacecraft and upper stages, the latter are typically better candidates for removal.

Let consider, for example, the sun-synchronous regime, where approximately 20% of the new launches are carried out. Being the orbital inclinations fixed around 98° by the sun-synchronicity requirement, at the same mean altitude h the "critical" debris flux F only depends on the target mass M. For h = 800 km, F(900 kg) $\cong$ 1.88 $\times F$(9000 kg), according to the ESA's MASTER-2009 model [12], so the application of Eq. (4) leads to the conclusion that the removal of a single 9 metric tons object is equivalent to the removal, in the same region of space, of about 30 "average" targets of 900 kg. This also means that a single active removal mission targeted at a high mass object may be more beneficial, over the long-term, than a multiple removal mission targeted at several "average" objects, additionally penalized by much more complex and lengthy operations.

Based on the available information [1][13][14][15][16][17], there are currently 25 unclassified abandoned objects with $M \geq$ 4000 kg orbiting the Earth in nearly circular orbits with 700 km $\leq h \leq$ 1100 km (Table 1). They represent just 1.1% of the spacecraft and upper stages in LEO, but approximately 10% of the mass (ISS excluded). Only one of them is a spacecraft, Envisat, suddenly lost by ESA on 8 April 2012 due to a critical failure; all the other are massive spent rocket bodies, 4 from China and 20 from Soviet Union/Ukraine/Russia. The Envisat spacecraft, the 4 Chinese upper stages and 2 of the Zenit rocket second stages are placed in sun-synchronous orbits, while the other 18 Zenit second stages are in orbits with inclination of about 71°. All the objects have a residual orbital lifetime of about one century or more, so they represent a potential and significant long-term source of fragmentation debris mass in two altitude-inclination bands already characterized by the maximum densities of artificial objects [7]. Therefore, also for the reasons previously discussed, they might represent the best targets to start active object removal in LEO.

Table 1 also shows the impactor minimum masses needed to fully destroy the listed objects, and the resulting number of debris larger than 10 cm according to Eq. (2). The impactor minimum masses were estimated assuming an energy-to-mass ratio threshold for catastrophic fragmentation of 40,000 J/kg, based on tests and analyses carried out in the past [18]. Actually, passivated rocket bodies might be more impervious to catastrophic fragmentation by 50%, but stages not passivated (and this is the case of most, if not all, the upper stages listed in Table 1) might be significantly more vulnerable to breakups, so the standard value, i.e. 40,000 J/kg, was applied to all the objects. In any case, it should be remarked that a single catastrophic fragmentation involving Envisat or a Zenit second stage would increase the total number of cataloged fragments in orbit around the Earth by 40%, with an even more dramatic relative impact in LEO, in particular below 1000 km.

Table 1: Spacecraft and rocket bodies with $M \geq 4000$ kg and $700\ \text{km} \leq h \leq 1100$ km

Object	**No.**	**Dry Mass (kg)**	**Mean Altitude (km)**	**Inclination (°)**	**Mass of Critical Impactor (kg)**	**Catastrophic Breakup Fragments ≥ 10 cm**
CZ-2C 2nd stage	3	4000	727 - 827	98.1 - 98.3	1.6	2580
CZ-2D 2nd stage	1	6000	817	98.3	2.5	3496
Envisat	1	7800	767	98.4	2.8	4258
Zenit 2nd stage	18	8900	829 - 851	71	3.6	4702
Zenit 2nd stage	2	8900	808 - 996	98.3 - 99.1	3.6	4702

Table 2: Relative ranking for active object removal compared to an average target of 934 kg placed into the same orbit of Envisat

Object	**No.**	**Mean Altitude (km)**	**Inclination (°)**	**Mass Ratio**	**Critical Impactor Flux Ratio**	**Removal Relative Ranking**
CZ-2C 2nd stage	3	727 - 827	98.1 - 98.3	4.28	0.44	5.6
CZ-2D 2nd stage	1	817	98.3	6.42	0.40	10.4
Envisat	1	767	98.4	8.35	0.60	24.6
Zenit 2nd stage	18	829 - 851	71	9.53	0.34	17.6
Zenit 2nd stage	2	808 - 996	98.3 - 99.1	9.53	0.32	16.5

Taking as reference (R = 1) an "average" object of 934 kg abandoned in the same orbit of Envisat and computing the flux of critical impactors with MASTER-2009 [12], the relative ranking for active removal, according to Eq. (4), of the massive objects listed in Table 1 is presented in Table 2. Envisat is the highest priority target, with a ranking equivalent to the removal of nearly 25 average objects with similar orbits. It is followed by the 20 Zenit rocket second stages, whose total ranking is equivalent to that of about 350 average targets, while the 4 Chinese rocket bodies together correspond to 27 average targets, so are almost equivalent to Envisat. Taken together, the 25 massive objects of Tables 1 and 2 have therefore a ranking equivalent to that of more than 400 average targets.

3. Mission concept

The removal mission concept under study relies on capturing a pre-selected large debris, which is then de-orbited by exploiting the HPM on board the chaser spacecraft. Once the chaser has approached the target debris with a rendezvous maneuver, debris capture is performed with a system that allows a safe and robust mating of the chaser with the debris. At this point the HPM is ignited to start controlled de-orbiting and reentry. Hence, the following mission phases can be identified:

- chaser launch and rendezvous with the preselected debris
- debris capture and mating
- mated configuration controlled de-orbiting

The HPM is designed so to include all the avionics needed for mated configuration attitude control during de-orbiting.

3.1 De-orbiting analysis

Based on preliminary mission design it is expected that a large massive debris is captured by the chaser. The mated configuration is then de-orbited by using the HPM on board the chaser. Due to the large size and mass of the debris being de-orbited, the destruction process in the atmosphere is expected to be incomplete, so that the residual risk for ground population might be too high. Therefore, the reentry shall be controlled and directed to a specific location on the ground (usually uninhabited ocean regions). More specifically, based on previous studies on LEO de-orbiting strategies [19], the reentry is performed by steering the debris to an elliptical transfer orbit with a perigee sufficiently low so to allow its immediate atmospheric capture. In addition, to limit the ground impact area of fragments which survive the atmospheric heating, a sufficiently steep atmospheric incidence angle is used.

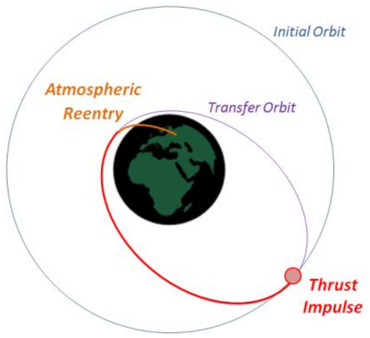

Figure 1: De-orbiting strategy illustration (one-burn case)

In this perspective, a preliminary, non-optimized, de-orbiting analysis is performed by assuming an elliptical reentry orbit with a perigee altitude of about 50 km and a flight path angle at 120 km lower than −1.5°. Figure 1 depicts the envisaged de-orbiting strategy. To steer the debris from its initial orbit to the elliptical transfer orbit both single burn and multi-burn strategies are investigated, even though in the considered case the number of burns shall be limited to allow an immediate reentry, so to relax the attitude control requirements of the mated configuration [19]. Indeed, below 300 km the atmospheric torque can significantly affect the controlled reentry maneuver [19]. Thrust levels and thrusting times relevant to the two strategies are shown in Table 3.

Table 3: De-orbiting strategiesparameters

	First-burn Thrust level (kN)	Second-burn Thrust level (kN)	First-burn Thrusting time (s)	Second-burn Thrusting time (s)
One-burn strategy	42	-	46	-
Two-burn strategy	13.7	13.2	86	86

A multiple-burn strategy (the two burns are separated by about 17 minutes) allows exploiting lower thrust levels, thus reducing the risk of debris fragmentation and docking system breakup. The ΔV needed for de-orbiting, estimated using the two-body model and a Hohmann transfer orbit, is about 250 m/s (25% margin included). This value is used for HPM and overall chaser satellite sizing.

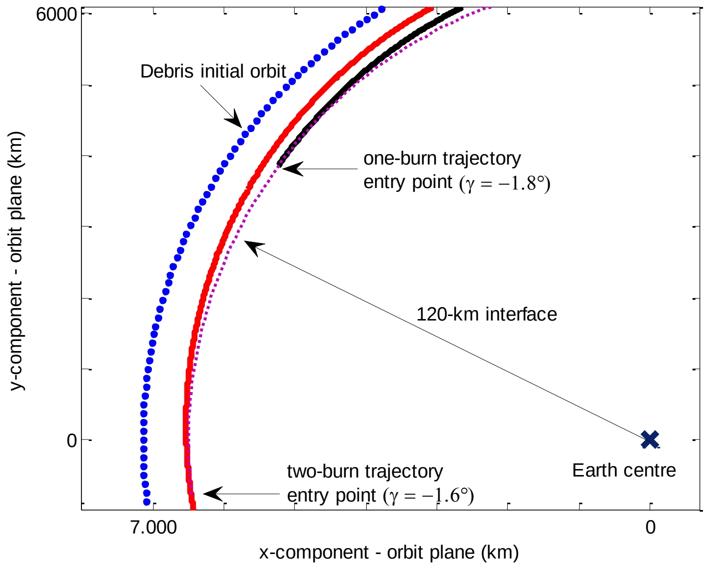

Figure 2: De-orbiting trajectories near the 120-km interface

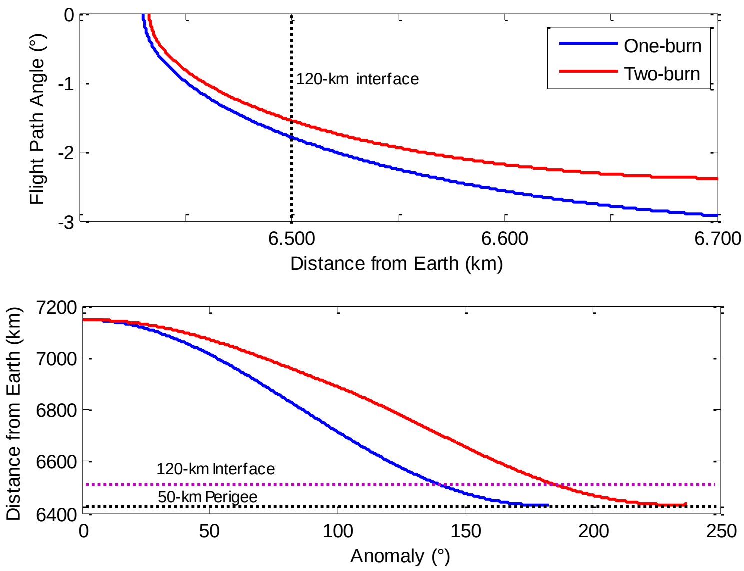

Figure 3: Fight path angleand perigee altitude for the two de-orbiting maneuvers

Figure 2 shows the simulated trajectories relevant to the two de-orbiting strategies. In the figure, to improve the results understanding, only the transfer trajectory segments near the 120-km interface are shown. From Figure 3 it can be seen that the resulting flight path angles of the one-burn and two-burn trajectories at the 120-km interface are about −1.8° and −1.6°, respectively; values compliant with the requirement of a steep re-entry strategy. It shall be outlined that the simulations refer to the de-orbiting of a 8000 kg object at 768 km altitude, like Envisat, and adopt preliminary results of HPM and chaser sizing and mass budget, presented in the next sections.

3.2 Rendezvous analysis

Rendezvous (RV) operations shall bring the chaser to its final state relative to the debris, allowing capture and docking. In this section, an overview of the various phases of the RV is provided, together with a preliminary identification of the involved technologies and related critical issues. For a preliminary investigation of the rendezvous operations, it is assumed that the chaser is injected directly into the selected debris orbit plane in a lower altitude parking orbit. By exploiting the different orbital periods, phasing with the debris is achieved so to start the rendezvous maneuver, which reduces to a few tens of kilometers the separation of the chaser from the target expected location. This last one is known with an error up to 1-2 km, due to uncertainty in ground tracking and available Two-Line Elements (TLE) data set, which, as well known, are updated at prefixed time intervals [20]. Before starting far/mid-range RV, the actual position of the debris shall be determined by using optical sensors and IR sensors, to guarantee continuous coverage also during eclipse conditions, on board the chaser, such as a far range camera or a star sensor. Specifically, at this stage the most important information coming from the far range sensor is the Line-Of-Sight (LOS) to the target, in order to correctly drive the approach maneuver. Indeed, in this phase, angle-only relative navigation can be performed, starting from a coarse a priori relative orbit determination based on the knowledge of debris TLE data and service platform absolute orbit from a GPS receiver. Optical systems also allow a preliminary positive identification of the debris. Technology for far/mid range rendezvous should not represent a critical issue for the mission. Indeed, relevant hardware and methodologies could be inherited from already own space missions, like Orbital Express [21] and the more recent PRISMA [22], which successfully demonstrated in flight autonomous rendezvous and docking starting from distances up to a few hundreds of kilometers.

Table 4: RV phases summary

Phase	Operation	Sensors	Final range to Debris
Phasing	Debris phasing. Absolute navigation	GPS	~10 km
Far/Mid Range RV	Debris tracking and preliminary identification. Relative navigation	Far/Mid range optical/IR cameras	~10 m
Close-range RV	Debris fly-around for identification and inspection. Close proximity relative navigation	LIDAR, close range cameras	~1 m

Based on the relative position information, the chaser can be maneuvered to gradually approach the target. Specifically, the far/mid-range rendezvous maneuver has to bring the chaser to a close proximity of the target to start close-range rendezvous and then target capture with the methodology and the system described in the following section. When the separation from the target reduces to about a few meters, close range rendezvous is started and target relative position and attitude (pose) are determined. Close-proximity relative navigation poses significant technology challenges, since pose determination techniques for non-cooperative targets shall be implemented. To this end several technologies can be exploited. A LIDAR (Light Detection and Ranging) would produce a 3-D point cloud, which is then matched to an onboard model of the debris to estimate the pose with 3-σ errors of about 1° in LOS, 1% in relative range and about 5° in relative attitude. Onboard close range cameras can be used for target monitoring in order to identify it and discover possible external structural damages. Indeed, these last ones may prevent determining the debris pose with sufficient accuracy for final approach and capture. Onboard cameras can be also used for pose determination by exploiting monocular or stereo-vision techniques [23]. Techniques and algorithms capable of extracting natural features of the target with good invariance to lighting conditions (e.g. lines and edges), such as binarization, contour mapping, and edge detection, could be used to set up the synthetic information that will be used to determine the relative pose [24][25][26]. To this end, algorithms as target edge and 3D information matching relevant to monocular and binocular vision techniques, respectively, can be used. Also in this case, although to a smaller extent, hardware and methodologies could be inherited from already known rendezvous technology demonstration missions [21][22]. Due to the lack of robustness of pose measurements in space, and to cover measurements outages, dynamics filtering schemes can be used which rely on linear or non-linear models of the relative orbital dynamics [27].This could also allow the implementation of effective collision avoidance maneuvers before capture. Before starting final approach for capture, a target fly around is performed for its final positive identification and inspection prior capture. This phase brings to the identification of the best points for capture, as well. Table 4 summarizes the several phases of the rendezvous operations, together with the technological and methodological aspects.

4. Debris capture and mating

The debris capture strategy is based upon the employment of two grasping systems which operate in sequence: the first one (Soft Docking System) is in charge of establishing the initial contact with the object, damping the impact loads and compensating for the residual chaser-target relative attitude motion at the end of the rendezvous phase; the second one (Hard Docking System) is committed to realize a strong structural connection between the chaser and the debris, in order to withstand the propulsive loads during the de-orbiting maneuver.On one hand, the Soft Docking System (Figure 4 [7][28][29]) exploits electrostatic adhesion to generate the requested contact forces between the target surface and flexible electrodes mounted on a deformable material substrate which guarantees a better adaptability and adhesion between the interfaces. A secondary component of the system is made of low rigidity passive damping joints which reduce impact forces and dissipate the relative velocities and oscillations between the debris and the chaser vehicle after contact. The joints are based on elastomeric elements whose deformation determines internal energy dissipation.
The main advantage of the proposed Soft Docking System is that the adhesion mechanism does not require any particular structural feature to perform the grasping: in case of rocket bodies it could fit to the surface of the divergent part of the nozzle, and in case of abandoned spacecraft it could fit to any external surface of the vehicle.

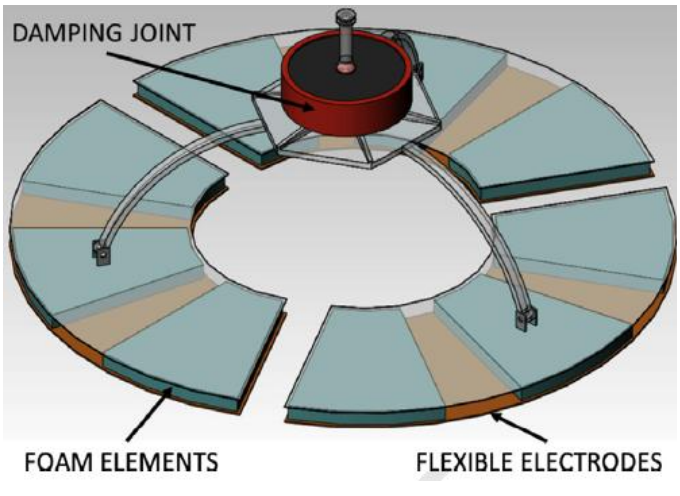

Figure 4: Soft docking system schematic

On the other hand, the Hard Docking System design is more dependent on the target: in case of abandoned rocket bodies, the gas dynamic nozzle may represent a good point for the chaser connection, due to its high resistance to thermal, fluid dynamic and mechanical strain. The chaser can be therefore equipped with a special “corkscrew system” (see Figure 5), theoretically able to secure the propulsion unit, hence the chaser, to the debris [30].
The corkscrew system is composed by a special titanium rod, which must be inserted inside the nozzle, centering the throat. The chaser must lean against the divergent nozzle border where the Soft Docking System connects to it. After completing the relative motion damping, the corkscrew mechanism can be activated, performing the mating with the internal walls of the convergent part of the nozzle. The mechanism consists of a threaded rod which moves four metal arms by cogwheels. This solution allows to enter through the small throat diameter, thanks to the initial forward orientation of the arms. Then, activated by electric actuators, the four metal arms rotates back toward the

internal convergent wall. At this point, the arms feet do not touch yet the nozzle surface (the erosion level of the wall is not known), thus a further rotation of only the head-end of the rode allow the arms feet to lean against the internal wall, involving a little compression of the nozzle, in order to keep it strictly connected to the chaser.

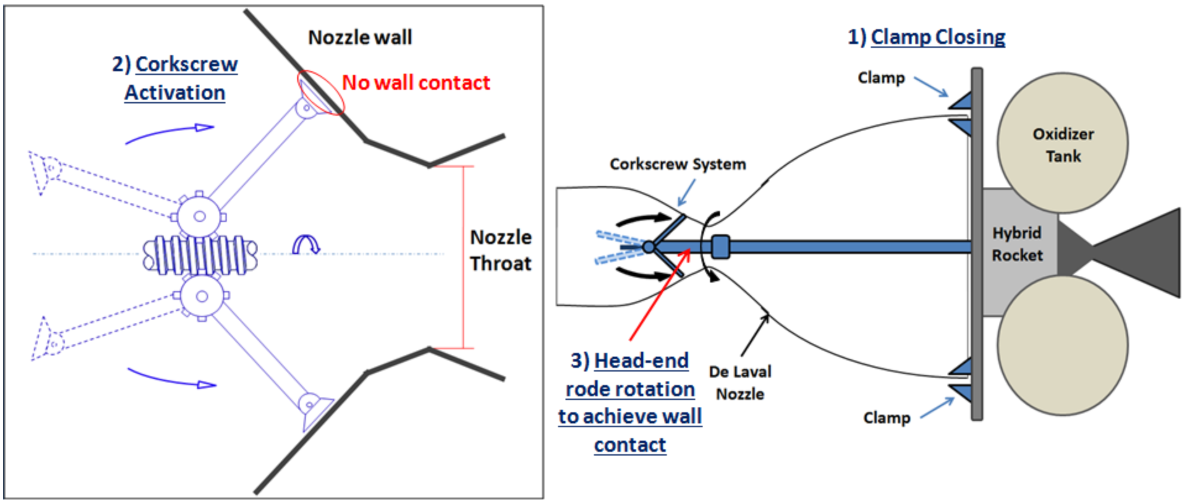

Figure 5: Corkscrew system mechanism

Differently from rocket bodies, abandoned spacecraft could be hard docked on the launcher cone adaptor or other structural panels, by means of a dedicated micro-driller mechanism that could be placed on the central part of the Soft Docking System, at the bottom of damping joint. The system will realize a stiff and safe mechanical link between the chaser and the target after soft docking is completed. It will place metal inserts on aluminum and/or composite plates and sandwich panels with a controlled drilling action which avoids dangerous damage on the target object (e.g. batteries and pressure vessels).
In summary, starting from the contact time instant, the capture procedure occurs as following. At the beginning of the capture sequence, the adhesive material is activated and put in contact with the debris surface. The polymeric foam substrate adapts to the local features of the target, the attraction force is established and the two bodies are softly connected. Preliminary estimations show that attraction pressures up to 10kPa normally and up to 4kPa in shear are feasible. In this phase the damping joint plays a key role in reducing the impulsive loads in the systems, thus reducing the requisites of the adhesion system and increasing the chances of a successful docking. In the next phase, the two objects move together with a residual relative velocity. The damping joint dissipates the relative kinetic energy and the oscillations decay over time. After the relative motion is completely damped, the chaser attitude control system de-tumble the two body system. When the angular momentum is completely dumped, the system attitude is stabilized and hard docking the chaser to the debris becomes possible.

5. HPM sizing and chaser mass budget

5.1 Hybrid propulsion module

The target size, the disposal strategy and the propulsion technology are important aspects with a strong impact on mass budget, system volume, and cost of the propulsion unit. Considering a large massive object, the capability of throttling and re-ignition may represent a stringent requirement for the adequate control of the disposing maneuver, whereas compact design is important for easier docking to the target and for dynamic stability of the final assembly (chaser and target). Compact volume may request a higher average propellant density but may collide with ΔV requirements for a controlled atmospheric reentry, needed by large systems, orbiting at the highest altitudes. Thrust level should stem from a trade-off choice about the risk of debris fragmentation, especially for large satellites, and long mission duration (correlated to propellant storability and collision risk during maneuver). Several innovative proposals are under development nowadays with varying time frames of realization; however, most of them need in-orbit demonstration of reliability and applicability on a real mission.
Out of this group, it is worth mentioning the use of tethers, as single spaceships as well as in fleet, to perform uncontrolled de-orbiting even of multiple targets[31][32]. Other options, for the time being, appeal to systems already studied or realized in on-board de-orbiting devices, such as drag augmentation techniques (deployed sails or inflating balloons) or proven propulsion devices [33]. In this respect, a cost analysis for the de-orbiting of a 1.2

metric ton IRS-1C satellite was presented for different propulsion options, suggesting that chemical rockets can be a viable solution [34]. Among this pool of technologies, solid propellants represent a simple, reliable, and proven technology but feature low specific impulse, limited flexibility and not suitability for multi-burn missions, while liquid propellants fill the gaps left by the solid propellants, but larger volumes and higher degree of complexity are requested. Furthermore, storability of the propellant must be carefully considered, as well as the high toxicity of typical liquid substances used for space applications. Thus, hybrid rocket technology for de-orbiting applications is considered a valuable option due to the high specific impulse obtainable, intrinsic safety, possibility of green propellant use, low cost technology and, especially, re-ignition and thrust throttleability. The latter may be a key aspect to avoid the risk of fragmentation for the most fragile components of a large abandoned satellite, during the de-orbiting maneuver.

A hybrid rocket engine typically features the oxidizer in the liquid or gaseous state, while the fuel is in the solid state. Its safety is guaranteed by no-contact between fuel and oxidizer, except during the combustion phase. A hybrid rocket can also be built with a particular geometry, using a tangentially oxidizer injection, resulting very compact and highly efficient in combustion, thanks to the oxidizer flow which provides a vortex combustion. This particular kind of engine results very small in size. Such characteristics can be the right solution for space debris mitigation, by supplementing with this engine the new satellites that will reach space in the future. In our view, this technology is very promising even in the field of space debris remediation, making possible the active removal in LEO of large intact objects (several metric tons), both spacecrafts and rocket bodies, by using one HPM for the reentry maneuver, equipped with several micro-thrusters, for the attitude control, spilling the HPM liquid oxidizer and burning it as a monopropellant (dual-mode use) [7][35][36][37]. Overall, a hybrid propulsion module represents a solution that mediates benefits and drawbacks from both liquid and solid rocket technology. On one side, it is bestowed the throttleability and re-ignition capability typical of liquids, specific impulse levels which fall in between the performance of solid and liquid propulsion, and a higher mean propellant density due to the use of a solid fuel. Nevertheless, a technological gap exists due to late development and lack of in-orbit demonstration.

In the simplest possible configuration, a hybrid rocket is made by a center-perforated solid fuel placed in the combustion chamber where an injector blows in a liquid or gaseous oxidizer. Low regression rate is the main drawback of this combustion process, but different means are considered for the enhancement of mass burning rate spanning from the use of advanced additives to different injection approaches (swirling oxidizer and vortex combustion) [38][39]. Moreover, special advanced designs of the combustion chamber, such as vortex pancake, provides high combustion efficiency, low performance variation during combustion, and – in the case of solid metal additives – reduced emission of condensed combustion products thanks to the vortex effect [40].

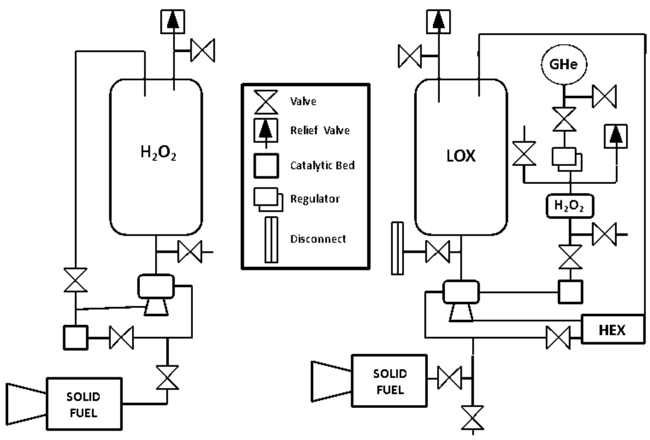

Figure 6: Comparison between H_2O_2 and LOX engine cycle complexity[7]

For the preliminary sizing of the HPM, the attention is focused on HTPB (hydroxyl-terminated polybutadiene) as fuel and H_2O_2 as oxidizers. This combination of propellants provides ideal vacuum specific impulses ($I_{s\text{-}vac}$) over 300 s and significant volumetric specific impulses (I_v), due to the high density of the hydrogen peroxide [7]. In view of its good compromise between performance, costs and toxicity, hydrogen peroxide seems to be the best choice for this kind of application. In particular its catalytic decomposition provides oxygen-rich hot gases up to 1,000 K. Considering that ignition of HTPB solid fuel requires about 800 K, it is possible to develop a simple and reliable re-ignition system. Moreover, with a single tank of H_2O_2, it is possible to feed both the primary propulsion system and a set of Reaction Control System (RCS) catalytic micro-thrusters. Though hydrogen peroxide is notorious for its storability issues, due to its decomposition inside tanks, high level of peroxide purity and the use of appropriate materials have demonstrated that risks can be avoided and the rate of dissociation can be reduced appreciably [41].

Hybrid technology allows to manage the thrust level, by the supply of oxidizer mass flow rate, providing gradual accelerations during the initial transient phase. In fact, while for a rocket body, due to its structural design, the risk of fragmentation is low, a spacecraft, made by thin and light structures, having several appendages (i.e. antennas, solar panels, etc.), requires to be stressed by low accelerations, in order to avoid any possible breakup and the consequent generation of new debris. Controlled de-orbiting of a large abandoned spacecraftor rocket body can requires a ΔV between 200 m/s and 450 m/s, depending on the target's initial orbit and the type of transfer maneuver [19]. For a large debris in LEO, like Envisat, according to the strategy previously discussed, a ΔV of 200 m/s is estimated for de-orbiting. In order to take into account the low combustion efficiency and the ignition transients, the required ΔV has been increased by 25%. Proper experiments about combustion configurations and engine firing tests will provide the effective performance parameters for different injection and geometrical chamber design solutions.

Considering a semi-impulsive maneuver, to provide a velocity increment of 250 m/s (200 m/s + 25%), a HPM is necessary with a mass of about 1010 kg, with a single central perforation solid fuel grain. Nevertheless, with this approach the thrust level results very high, ~40 kN, with an average acceleration of 0.45g on the system (chaser + debris). The mass of propellant is enough to perform even the rendezvous maneuver, starting from 700 km with an Hohmann transfer requiring about 45 m/s (36 m/s + 25%), by two impulse of thrust. This HPM results with a diameter of 34 cm and a total length (including submerged nozzle) of 251 cm. The high thrust generated, using this maneuver approach, could be dangerous and not supportable by the Envisat's structure. At this preliminary phase, it is difficult to predict the appropriate thrust profile without a detailed flight dynamic analysis of the disposal maneuver for such a large object. However, supposing to provide the required velocity increment with two burns, each one lasting about 86 s, the thrust level generated is significantly lower, lesser than 13 kN with an average acceleration of 0.15g on the system. In this case the HPM has a mass of 896 kg, due to lower operative chamber pressures, low oxidizer mass flow rates and, consequently, lower thickness for engine structural components. Even the length of the solid fuel has been reduced and the fuel web thickness increased, requiring a lower thrust level for longer burn times. The external diameter of this HPM is 37 cm, while the total length (including submerged nozzle) is 206 cm.

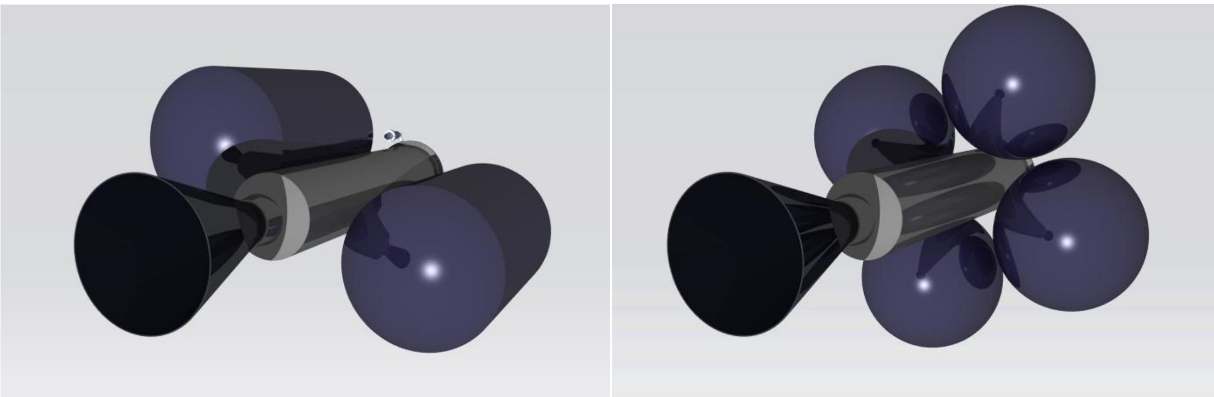

Figure 7: HPM conceptual sketch with 2 cylindrical tanks configuration (left) and 4 spherical tanks configuration (right)

If the oxidizer tanks are placed at the sides of the rocket, the final HPM diameter will be about 188 cm (for both HPM considered). The $I_{s\text{-}vac}$results about 310 s. For a better mass distribution and a more compact configuration, four spherical tanks, having an external diameter of about 77 cm, with an internal elastomeric membrane for pressurization with gaseous N_2, are considered. However, with the aim of cost lowering, two lateral cylindrical tanks would be preferable.

Then the ignition of the primary propulsion system is performed by catalytic cells in which the hydrogen peroxide decomposes generating oxygen-rich hot gases, then expanded in the combustion chamber. In order to limit the hydrogen peroxide natural decomposition, hence hazard risk, high purity aluminum tanks are recommended [42]. This HPM sizing takes into account even the mass of a RCS system for attitude control of the rendezvous maneuver, debris capture and de-orbiting disposal. Because of the increase of oxidizer to fuel ratio (O/F) during the combustion, hence oxygen-rich exhaust gases, a nozzle made by phenolic material is preferable, due to its better resistance than graphite. A cooling system for the nozzle will be considered in a more advanced design phase, depending on the combustion time required by the disposal maneuver optimization.

5.2 System mass budget

A preliminary mass estimate for the chaser is performed to the aim of RV and de-orbiting analysis and HPM sizing. It is carried out with reference to the removal of one large massive object of about 8000 kg in a 768-km orbit, like Envisat. The chaser mass budget is computed starting from the estimated ΔVs for rendezvous/docking and de-orbiting. More specifically, the chaser initial mass is estimated from the knowledge of the Mass Ratios (MR) relevant to the two maneuvers. For a preliminary estimate of the ΔV needed for the rendezvous with the debris, a launch with VEGA is assumed. However, different launchers could be included in the analysis as well. Considering the VEGA required nominal performance [43], it is assumed that the chaser is injected directly into the debris nominal orbit plane in a 700-km parking orbit. Thus, assuming the two-body model and Hohmann transfer orbits, the mass ratio relevant to the *i-th* maneuver, MR_i, can be expressed as function of the corresponding ΔV_i as follows:

$$MR_i = e^{\Delta V_i / I_{sp} g} \tag{5}$$

where I_{sp} and g are the specific impulse and the gravity acceleration, respectively. As discussed in the previous sections, the values estimated for the ΔVs of the rendezvous (ΔV_1) and de-orbiting (ΔV_2) maneuvers are 45 m/s and 250 m/s (25% margin included [44]), respectively. This, considering a specific impulse, I_{sp}, of about 310 s, yields the values of about 1.015 and 1.085 for the corresponding mass ratios, MR_1 and MR_2. Hence, the ratio of the propellant consumption to the initial mass for each maneuver can be expressed according to the following equations:

$$\frac{mp_1}{m_{in}} = 1 - \frac{1}{MR_1} = 1 - e^{-\Delta V_1 / I_{sp} g} \tag{6}$$

$$\frac{mp_2}{m_{in1}} = 1 - \frac{1}{MR_2} = 1 - e^{-\Delta V_2 / I_{sp} g} \tag{7}$$

where m_{in} is the chaser initial mass including the chaser bus mass (i.e. subsystems, structure, mechanisms), m_{bus}, the HPM mass (only the inert fraction), m_{HPM}, the propellant mass needed to perform the rendezvous and docking maneuver, m_{p1}, and the propellant mass required by the de-orbiting maneuver, m_{p2}. Thus, we have:

$$m_{in} = m_{bus} + m_{HPM} + m_{p1} + m_{p2} \tag{8}$$

Instead, m_{in1} in Eq. (7) is the mass of the chaser-debris mated system at the beginning of the de-orbiting maneuver, i.e.:

$$m_{in1} = m_{in} + m_{debris} - m_{p1} \tag{9}$$

where m_{debris} is the debris mass. For preliminary mass budget, the HPM inert mass, m_{HPM} , is expressed as a percentage of HPM total mass, and then of the propellant mass, as follows:

$$m_{HPM} = k_1(m_{HPM} + m_{p1} + m_{p2}) = \frac{k_1}{1-k_1}(m_{p1} + m_{p2}) = k(m_{p1} + m_{p2}) \tag{10}$$

By using Eq. (6), (7), (9) and (10), after some mathematics, Eq. (8) can be re-written as follows:

$$m_{in} = \frac{MR_1 MR_2 m_{bus} + MR_1(k+1)(MR_2-1)m_{Debris}}{[1-k(MR_1 MR_2 - 1)]} \tag{11}$$

which yields the chaser initial mass as a function of the bus and debris mass. Since the chaser has to carry in orbit all the avionics needed for mission operation and debris rendezvous and capture, from preliminary system consideration and historical data relevant to autonomous rendezvous demonstration missions [20][21], the bus mass can be estimated in the range 500–700 kg. Hence, considering typical values for k_1 (i.e. 0.2–0.3), the chaser initial mass can be computed as:

$$m_{in} = 1.101 m_{bus} + 912 \tag{12}$$

This yields a chaser initial mass value in the range 1460÷1680 kg (about 20% of the removed mass), which is very close to the value that can be computed after HPM sizing and to the VEGA limiting performance.

6. Conclusions

In this paper the active removal of a large massive debris from LEO, by exploiting hybrid propulsion technology, was investigated. A demonstration mission concept was developed in which, following debris target identification, rendezvous and capture, a hard docking system is used for a solid structural connection between the target and the chaser, equipped with a hybrid propulsion module. The operational flexibility of the hybrid propulsion system allows indeed to perform both the rendezvous with the selected object and a controlled de-orbiting and atmospheric re-entry. For the preliminary analysis of the various technologies involved in a removal mission, a target debris having Envisat characteristics, in terms of mass, size and orbit, was considered. Critical issues relevant to the debris active removal system were investigated at a preliminary stage, with particular attention to debris controlled de-orbiting, possible approaches and technologies for rendezvous, capture and mating and hybrid propulsion module sizing, as well as the chaser vehicle preliminary mass budget. Owing to the non-cooperative nature of the target, a mission critical aspect surely is debris capture. A two-stage capture strategy was proposed in the paper, relying on soft and hard docking systems operating in sequence. In particular, an innovative concept based on the electro-adhesive soft docking was introduced, allowing impact load damping and compensation of the residual relative attitude motion between the non-cooperating target and the chaser. This solution should allow high flexibility in the capture point selection and high adaptability to the debris surface. After debris capture, and before engine ignition, a rigid structural connection of the chaser vehicle with the target has to be established to allow complete control of the mated configuration during de-orbiting. To this end, a hard docking mechanism, like the corkscrew system suitable for nozzle of abandoned launcher upper stages and adapted to abandoned spacecrafts, was considered. For the hybrid propulsion module sizing, different design solutions were compared, depending on the disposal strategy characteristics. In fact, a low thrust multi-burn strategy would be more suitable for a successful and safe removal of a large massive debris, especially if its structure is fragile and provided with several appendages (i.e. solar panels, antenna etc.). However, at the same time, the flight path angle at the re-entry interface was maintained sufficiently steep, and the number of burns was limited to allow an immediate atmospheric capture and a ground impact within a pre-specified area. The mass budget of the chaser spacecraft was also performed to investigate its compatibility with a VEGA launch. Preliminary estimates show that the chaser mass ranges between 1500 kg and 1700 kg, depending on the technologies exploited for the chaser bus, with the propulsion module weighting about 1000kg. These values are quite close, although still complying, to the VEGA limiting performance.

References

[1] Space Track Organization. 2013. Satellite Catalog Data. https://www.space-track.org.

[2] Union of Concerned Scientists. 2012. UCS Satellite Database 12-1-12. http://www.ucsusa.org.

[3] Anonymous. 2012. Monthly mass of cataloged objects in Earth orbit by object type. *Orbital Debris Quarterly News* 16(2):10.

[4] Liou, J.-C. 2011. An active debris removal parametric study for LEOenvironment remediation. *Advances in Space Research* 47:1865–1876.

[5] Anonymous. 2007. IADC space debris mitigation guidelines. Report IADC-02-01, rev. 1. Inter-Agency Space Debris Coordination Committee.

[6] Liou, J.-C., and N.L. Johnson. 2009. A sensitivity study of the effectiveness of activedebris removal in LEO. *Acta Astronautica* 64:236–243.

[7] De Luca, L.T., F. Bernelli, F. Maggi, P. Tadini, C. Pardini, L. Anselmo, M. Grassi, D. Pavarin, A. Francesconi, F. Branz, S. Chiesa, N. Viola, C. Bonnal, V. Trushlyakov, and I. Belokonov. 2013. Active space debris removal by a hybrid propulsion module. Acta Astronautica, doi: http://dx.doi.org/10.1016/j.actaastro.2013.04025.

[8] Utzmann, J., M. Oswald, S. Stabroth, P. Voigt, A. Wagner, and I. Retat. 2012. Ranking and characterization of heavy debris for active removal. In: *Proc. 63rd International Astronautical Congress*. DVD, ISSN 1995-6258. International Astronautical Federation. Paper IAC-12-A6.2.8.

[9] Johnson, N.L., P.H. Krisko, J.-C. Liou, and P.D. Anz-Meador. 2001. NASA's new breakup model of EVOLVE 4.0. *Advances in Space Research* 28:1377–1384.

[10] Krisko, P.H. 2011. Proper implementation of the 1998 NASA breakup model. *Orbital Debris Quarterly News* 15(4):4–5.

[11] Boden, D.G. 1996. Introduction to astrodynamics. In: *Space Mission Analysis and Design*. Second Edition. Microcosm Inc. & Kluwer Academic Publishers. 129–156.

[12] Institute of Aerospace Systems, TU Braunschweig. 2012. Meteoroid and space debris terrestrial environment reference model (MASTER-2009). Version 7.0.2 of 5 October 2012. European Space Agency.

[13] Bond, P.R. (Ed.). 2012. *IHS Jane's: Space Systems & Industry 2012-2013*. IHS Global Limited.

[14] Zak, A. 2013. Zenit second stage. *RussianSpaceWeb.com*. http://www.russianspaceweb.com/zenit_stage2.html
[15] China Great Wall Industry Corporation. 2013. LM-2C.http://www.cgwic.com/LaunchServices/LaunchVehicle/LM2C.html.
[16] China Great Wall Industry Corporation. 2013. LM-2C.http://www.cgwic.com/LaunchServices/LaunchVehicle/LM2D.html.
[17] Barbosa, R.C. 2013. China back in action with Long March 2D launch of Gaofen-1. *NASA Spaceflight.com*. http://www.nasaspaceflight.com/2013/04/china-back-in-action-long-march-2d-gaofen-1/.
[18] McKnight, D.S. 1993. Collision and breakup models: pedigree, regimes, and validation/verification. Briefing presented on November 18 to the National Research Council Committee on Space Debris Workshop, Irvine, California.
[19] Janovsky, R., M. Kassebom, H. Lubbersted, O. Romberg. 2002. End-Of-Life De-Orbiting Strategies for Satellites. In: DeutscherLuft- und Raumfahrtkongress. DGLR-JT2002-028.
[20] Pinson, R.M., et al. 2008. Orbital express advanced video guidance sensor: ground testing, flight 1049results and comparisons. In: Navigation and Control Conference and Exhibit. AIAA Guidance.
[21] Bodin, P., et al. 2009. PRISMA: an in orbit test bed for guidance, navigation, and control experiments. *J. Spacecraft Rockets*, Volume 46, pp. 615-623.
[22] Fasano, G., A. Accardo, and M. Grassi. 2009. A Stereo-vision Based System for Autonomous Navigation of an in-orbit Servicing Platform. AIAA Infotech@Aerospace. ISBN-10: 1-56347-971-0.
[23] Gonzalez, R.C., and Woods, R.E. 2008. Digital image processing. In: 3rd edition, Pearson International.
[24] Alferez, R., and Y.-F Wang. 2009. Geometric and illumination invariants for object recognition. *IEEE Transac. Pattern Anal Mach Intell.*, doi:10.1109/34.771318 1081.
[25] Sako, H., M. Whitehouse, A. Smith, and A. Sutherland. 1994. Real-time facial-feature tracking based on matching techniques and its applications. In: Proceedings of the 12th IAPR International Conference on Computer Vision and Image Processing, Pattern Recognition, Volume 2.
[26] Nishida, S., and T. Yoshigawa. 2003. Space debris capture by a joint compliance controlled robot. In: Proceedings of the 2003 IEEE/ASME International Conference on Advanced Intelligent Mechatronics.
[27] Accardo, D., G. Fasano, and M. Grassi. 2013. Vision-based Relative Navigation, Distributed Space Missions for Earth System Monitoring. Space Technology Library. Volume 31, pp. 267-305.
[28] Branz, F. et al. 2012. Innovative technologies for non-cooperative targets close inspection and grasping. In: 63rd IAC Congress.
[29] Branz, F. et al. 2013. Soft docking system for capture of irregularly shaped, uncontrolled space objects. In: 6th European Conference on Space Debris.
[30] Tadini, P., F. Maggi, L.T. DeLuca, C. Pardini, L. Anselmo, M. Grassi, V. Trushlyakov. 2012. Active Debris Removal of a Cosmos-3M second stage by Hybrid Rocket Module. In: VIII International Science and Technology Conference ”Dynamics of Systems, Mechanisms and Machines”.
[31] Bombardelli, C., et al. 2010. Electrodynamic tethers for space debris removal. In: Space Debris Mitigation Workshop.
[32] Ohkawa, Y., et al. 2012. Electrodynamic tether (edt) propulsion for LEO debris de-orbit. In: 2nd European Workshop on Active Debris Removal, CNES HQ.
[33] Trushlyakov, V. 2010. Development of means for space debris de-orbiting on the basis of separating parts of upper stages of the space launcher vehicle with liquid propulsion engine. In: Beijing Orbital Debris Mitigation Workshop.
[34] Burkhardt, H. et al. 2002. Evaluation of propulsion systems for satellite end of life de-orbiting. AIAA Paper 4208.
[35] DeLuca, L.T., et al. 2012. Active Space Debris Removal by Hybrid Propulsion Module, Research project proposal to the italian Ministry of Education, University and Research (MIUR).
[36] DeLuca, L.T., et al. 2012. Active space debris removal by hybrid rocket propulsion. In: Proceedings of the 2nd European Workshop on Active Debris Removal, CNES HQ.
[37] De Luca, L.T., F. Bernelli, F. Maggi, P. Tadini, C. Pardini, L. Anselmo, M. Grassi, D. Pavarin, A. Francesconi, F. Branz, S. Chiesa, N. Viola, C. Bonnal, V. Trushlyakov, and I. Belokonov. 2012. Active space debris removal by hybrid engine module. In: *Proc. 63rd International Astronautical Congress*. DVD, ISSN 1995-6258. International Astronautical Federation.Paper IAC-12-A6.5.8.
[38] Chiaverini, M.J., and K.K. Kuo. 2007. Fundamentals of Hybrid Rocket Combustion and Propulsion, AIAA Progress in Astronautics and Aeronautics, Volume 218, pp. 37-116, 457-485.
[39] Czysz, P., and C. Bruno. 2006. Future spacecraft propulsion systems: Enabling technologies for space exploration, Springer Praxis.
[40] Gibbon, D.M., and G.S. Haag. 2001. Investigation of an alternative geometry hybrid rocket for small orbit transfer, Report SPBB-26287-01. Surrey Satellite Technology Limited.

[41] Ventura, M., E. Wernimont, S. Heister, and S. Yuan. 2007. Rocket Grade Hydrogen Peroxide (RGHP) for use in Propulsion and Power Devices. Historical discussion of hazards. AIAA Paper 5468.
[42] Anonymous. 2010. Hydrogen peroxide (H2O2) safe storage and handling. Technical Information Papers and Useful Methods. TAPPI Standard TIP 0606-24, pp. 8.
[43] Anonymous. 2006. VEGA User Manual. Arianespace, Issue 3.
[44] Brown, C. 2002. Elements of Spacecraft Design. AIAA Education Series, American Institute of Aeronautics and Astronautics, Inc., ISBN: 978-1-60086-051-5.